Talanta 201 (2019) 46–51

Contents lists available at ScienceDirect

Talanta

journal homepage: www.elsevier.com/locate/talanta

Sensitive surface-enhanced Raman scattering detection of atrazine based on aggregation of silver nanoparticles modified carbon dots

Jianshe Tang[a,b], Weiwei Chen[a], Huanxian Ju[a,*]

[a] State Key Laboratory of Analytical Chemistry for Life Science, School of Chemistry and Chemical Engineering, Nanjing University, Nanjing, 210023, PR China
[b] Department of Environment and Energy Engineering, Anhui Jianzhu University, Hefei, 230601, PR China

ARTICLE INFO

Keywords:
SERS detection
Atrazine
Carbon dots
Target induced aggregation
Pesticides
Silver nanoparticles

ABSTRACT

The development of precise detection methods with simply operation for pesticides in various environmental samples is a particular challenge. Here a highly sensitive surface-enhanced Raman scattering (SERS) approach for the selective detection of trace atrazine was proposed with R6G as a Raman reporter, which was adsorbed on silver nanoparticles modified carbon dots. The latter were prepared by the reduction of Ag^+ by carbon dots. In the presence of atrazine, the aggregation of the modified carbon dots due to the interaction between silver nanoparticles and atrazine led to great enhancement of the SERS signal of R6G. Under optimal assay conditions, the limit of quantification was estimated to be 10 nM, which matched with the standard for drinking water quality of China and WHO defined limit. A good linear response to atrazine was found in the concentration range of 10–1000 nM with the relative standard deviations between 1.8% and 5.6%. The determination of atrazine in real water samples was also carried out to confirm the practicability of the proposed method, which showed the recoveries from 95% to 117.5%. The target induced aggregation for enhancing the signal offered great potential for sensitive on-site detection of atrazine in environments.

1. Introduction

Pesticides can increase the crop yield and enhance the quality of foods. Thus the use of pesticides is increased dramatically. However, indiscriminate use and misuse of pesticide cause the potential environmental hazards and/or food safe problems. Atrazine (2-chloro-4-ethylamino-6-isopropylamino-s-triazine) is a restricted-use herbicide manufactured, formulated, and sold under various trademarks by several agrochemical companies. It is most often used in corn, sorghum, and sugar cane production for the control of annual broadleaf and grass weeds [1]. Due to the low persistence of atrazine herbicide, repeated applications are practiced for the control of weeds in agricultural fields, and as a result, large quantities of the herbicide find their ways into water bodies [2]. Thus many traditional methods such as gas chromatography (GC) [3], high-performance liquid chromatography (HPLC) [4], mass spectroscopy (MS) [5], electrochemiluminescence [6], and voltammetric methods [7], have been used to measure the pesticide residues in foods. However, these methods face to many disadvantages, such as labor-intensive, time-consuming operation, and complicated sample pre-treatment [8]. In addition, the scarceness of a quick, easy, and economic detection method to detect pesticide residues in a complex matrix is a major hindrance for the environment and food safety [8]. The precise detection methods with simply operation for pesticides in various environmental samples is still a challenge.

Surface-enhanced Raman spectroscopy (SERS) is a viable technique for rapid viral detection in a nondestructive manner, with sensitivity down to single molecules [9]. SERS has many advantages compared to other conventional methods. For instance, the sample preparation for SERS is simple. Liquid samples can be measured directly on a SERS substrate. All of these features make SERS an ideal alternative method to detect chemical contaminants. Silver nanoparticles have been demonstrated as the most suitable substrate for SERS detection. Much attention has been focused on the size and shape-controlled synthesis of silver nanostructures [10]. Several Ag nanostructures, including particles [11], rods [12], wires [13], sheets [14], cubes [15], dendritic and flower-like structures [16], have been prepared with different methods. Some SERS methods based on the aggregation [17,18] and anti-aggregation [19] of Ag nanostructures have been developed for the determination of ions and proteases. Herein, we prepared for the first time the silver nanoparticles through reducing silver ion with carbon dots (CDs). The obtained silver nanoparticles modified CDs (CD@Ag) could be aggregated in the presence of atrazine due to the interaction between silver nanoparticles and atrazine. The aggregation led to the enhancement of both rhodamine 6G (R6G) adsorbed on the CD@Ag as a

* Corresponding author.
E-mail address: hxju@nju.edu.cn (H. Ju).

https://doi.org/10.1016/j.talanta.2019.03.108
Received 15 January 2019; Received in revised form 27 March 2019; Accepted 30 March 2019
Available online 01 April 2019

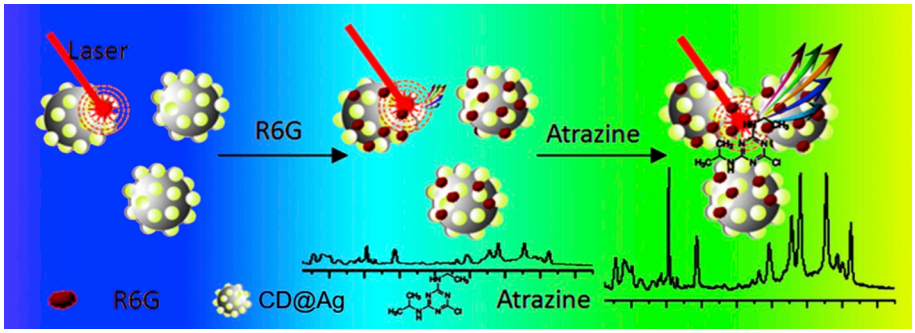

Fig. 1. Schematic diagram of the principle for atrazine assay based on the aggregation of CD@Ag induced by atrazine and R6G as a SERS reporter.

reporter and the Ag nanoparticles in local space, which increased the SERS signal and thus led to a convenient SERS method for sensitive analysis of atrazine (Fig. 1). The proposed SERS-based technology could be well applied to monitoring various targets by virtue of target-induced changes of nanoparticles stability.

2. Experimental

2.1. Materials and reagents

Silver nitrate, sucrose, ethylenediamine, R6G, 3-mercaptopropionic acid (MPA), and ethambutol (EB) were purchased from Sinopharm Chemical Co., Ltd. (Shanghai, China). Atrazine (> 98% pure) was purchased from China Agricultural Environment Protection and Inspection Center (Tianjin, China). All the reagents were of analytical-reagent grade and used as received, without further purification. Ultrapure water (> 18.0 MΩ cm) used in all experiments was purified using a Milli-Q gradient system (Millipore).

2.2. Preparation of carbon dots

CDs was prepared with sucrose according to the previously reported method [20]. Briefly, 3.0 g of sucrose and ethylenediamine (10:1) was added to 20 mL of ultrapure water at 90 °C, and the mixture solution was vigorously stirred for 30 min. Then the solution was transferred to a poly (tetrafluoroethylene) (Teflon)-lined autoclave and heated at 200 °C for 10 h. After the reaction, the reactor was cooled to room temperature by naturally.

2.3. Preparation of Ag nanoparticles modified CDs

In a typical preparation process, 0.5 mg of CDs was diluted by water (2 mL). Then 1 mL $AgNO_3$ (5 g/L) added into the solution. The mixture was heated by water bath. Subsequently, yellowish-brown nanoparticles were produced at room temperature within 120 min. The formed CD@Ag was then washed repeatedly with water for three times, and dried by freeze. Finally, the product was stored at 4 °C for later characterization and use [21].

2.4. Apparatus

Absorption measurements were performed using a Cary 60 ultraviolet–visible (UV–vis) spectrometer (Agilent Technologies, USA). Fluorescence spectra were recorded on a Cary Eclipse fluorescence spectrometer (Agilent Technologies, USA). Fourier transform infrared spectroscopy (FTIR) was conducted using KBr pellets and a PerkinElmer FTIR spectrophotometer (PerkinElmer, USA). Transmission electron microscopic (TEM) images were taken using a Tecnai G2 F20 transmission electron microscope (FEI, USA) operating at 200 kV. X-ray photoelectron spectroscopy (XPS) was performed using a Thermo ESCALAB 250Xi Multitechnique Surface Analysis spectrometer (Thermo, USA). SERS spectra were recorded using a confocal microscopic Raman spectrometer (Renishaw, UK). Scanning electron microscopic (SEM) images were obtained on environmental scanning electron microscope FEI Quanta 200 FEG (Philips, The Netherlands). The overall quantum yield was measured on FLS980 Edinburgh fluorescence spectrometer (Edinburgh, UK).

2.5. SERS detection of atrazine

For the detection of atrazine, a mixture of R6G, CD@Ag and atrazine was prepared, where atrazine was the aggregating agent. Several drops of the solution were spotted onto a quartz plate to measure the Raman signal with the Raman microscope equipped with a CCD detector with an excitation wavelength of 633 nm laser at 0.2 mW power. The laser beam was focused to a spot of about 1 mm^2 by a 50× microscope objective. The integral time was 2 s and the slit aperture was 25 mm.

2.6. Samples

Lake water samples (100 mL) were collected from the Yi Sea in Anhui Jianzhu University (Hefei, China) to verify the feasibility of the developed method. The representative lake water was filtered through 0.7 μm glass fiber filters (GF/F, Whatman), and spiked with atrazine to the final concentration of 5, 10, or 200 nM. All measurements were performed in triplicate.

3. Results and discussion

3.1. Syntheses and characterization of Ag nanoparticles modified CDs

The CDs were prepared with a hydrothermal synthesis method using the precursor of sucrose and ethylenediamine at a relative mole ratio of 10:1. The fluorescent character of CDs exhibited the maximum emission intensity at 410 nm at the excitation wavelength of 330 nm (Fig. S1a). The emission spectrum showed a highly excitation energy dependence: as the excitation wavelength was increased, the emission peak position shifted to longer wavelength and the intensity decreased (Fig. S1b). The obtained CD@Ag exhibited an apparently lower fluorescence intensity than CDs owing to the Förster resonance energy transfer (FRET) from CDs to silver nanoparticles as acceptor, which showed good overlap of the fluorescence emission spectrum of CDs with the absorption spectrum of silver nanoparticles (Fig. S1 c, d) [22,23].

The TEM image of the prepared CD@Ag indicated that the nanohybrids formed from the *in situ* reduction of silver ions by CDs protected and stabilized the Ag nanoparticles from aggregation, thus showed good dispersivity in aqueous medium (Fig. 2). The morphology of CD@Ag gave an approximate diameter of 5 nm and the ultrathin shell of silver nanoparticles was formed on CD core, which was different from that of AgNPs kernel coated by CDs prepared by using $NaBH_4$ as reductant [24]. The EDS spectrum of the as-prepared CD@Ag also

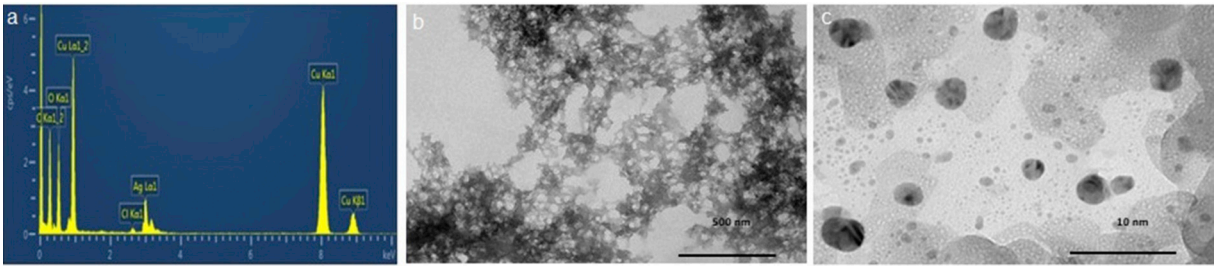

Fig. 2. EDS spectrum (a) and TEM images (b, c) of CD@Ag.

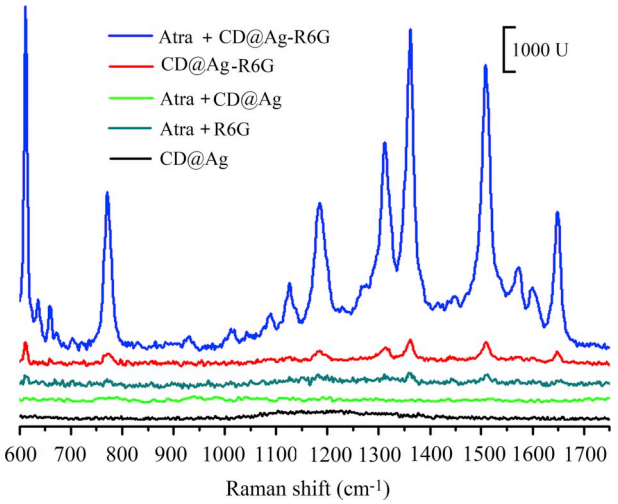

Fig. 3. SERS spectra of CD@Ag, CD@Ag-R6G, and the mixtures of atrazine with R6G, CD@Ag or CD@Ag-R6G.

suggested the successful coating of CDs by Ag nanoparticles (Fig. 2a), which showed the signals of only Ag, Cu and part of the C peaks resulting from the copper grid, demonstrating the high purity of the nanocomposites. The XPS spectrum was further performed to investigate the surface configuration, which exhibited the typical signals of C, O, N, and Ag (Fig. S2) for C1s at around 284.8 eV, O1s at 532.6, and Ag3d5/2 and Ag3d3/2 at 368.5 and 374.5 eV, respectively [25,26]. The peaks at 571 and 604 eV described the Ag3p3/2 and Ag3p1/2, indicating the formation of metallic Ag [27].

Size distribution analysis by DLS measurements indicated that the size of the prepared CD@Ag ranged from 1 to 10 nm, while it increased to 50–100 nm upon the presence of atrazine (Fig. S3), demonstrating the aggregation of CD@Ag induced by atrazine.

3.2. Principle of SERS sensing for atrazine

R6B, a commonly used Raman molecule, was selected as a reporter to perform the SERS detection, as shown in Fig. 1. Due to the atrazine-induced aggregation of CD@Ag, which was different from the aggregation of free silver nanoparticles [17,28], the amounts of both R6G and Ag nanoparticles in local space increased upon the addition of atrazine, which increased the SERS signal and produced a possible analytical method for SERS sensing of atrazine.

The CDs did not show obvious Raman response, while the Raman spectrum of CD@Ag exhibited weak peaks of carbon species. Probably, the Raman peak of CDs was annihilated by its fluorescence, while the fluorescence was quenched by silver nanoparticles in CD@Ag [29]. After R6G was adsorbed on CD@Ag to form CD@Ag-R6G, its Raman signals were obviously enhanced due to the localized surface plasmon resonance and/or near-field electromagnetic enhancement on the surface of CD@Ag (Fig. 3). The Raman spectrum showed typical peaks of R6G molecules at 611, 771, 1127, 1192, 1315, 1513, and 1652 cm^{-1}

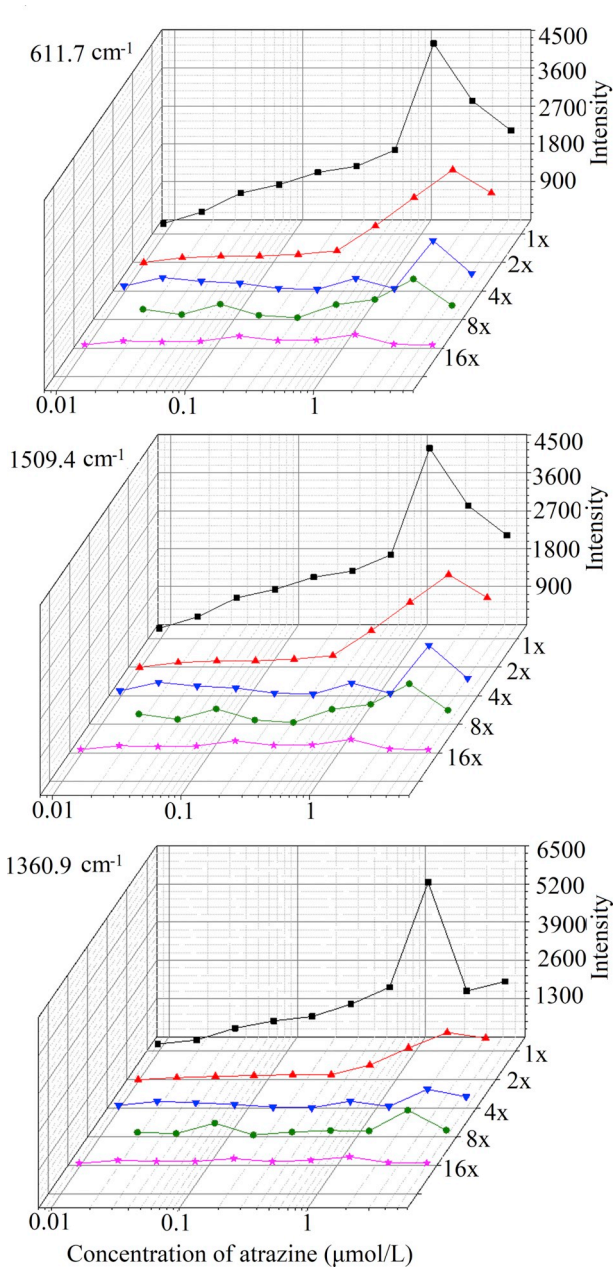

Fig. 4. SERS intensity of R6G enhanced by CD@Ag at the dilution times of 1, 2, 4 8 and 16 in the present of atrazine at different concentrations.

[30], in addition of the weak Raman bands at 567, 609, 1307, 1361 and 1509 cm^{-1}, which were in agreement with the results reported previously [31–36]. The peaks of R6G at 611, 1361 and 1509 cm^{-1} were attributed to C—C ring in-plane bending in xanthene/phenyl rings [31].

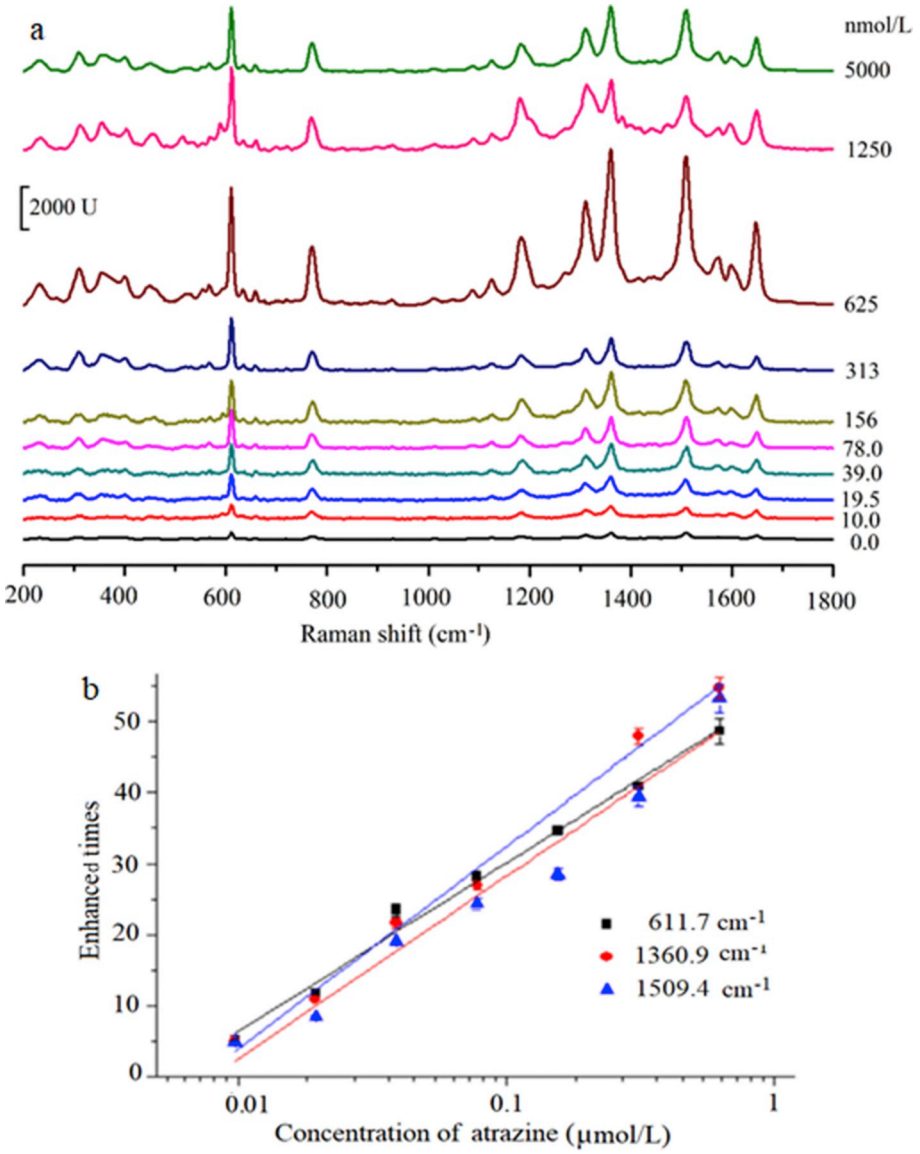

Fig. 5. Raman spectra of R6G enhanced by the accumulation of CD@Ag with atrazine ranging from 0.01 to 5 μmol/L (a), and calibration curves of atrazine in methanol solutions (b).

Table 1
Recoveries of atrazine from spiked environmental water samples (n = 10).

Peaks (cm^{-1})	Spiked (μmol/L)	Found (μmol/L)	Recovery (%)	SD (μmol/L)	CV (%)
1360	0.10	0.095	95	0.006	6.3
	0.02	0.022	110	0.0018	7.9
611	0.10	0.115	115	0.054	15
	0.02	0.022	110	0.003	13
1509	0.10	0.105	105	0.019	18
	0.02	0.0235	117.5	0.0024	10

The peak at 771 cm^{-1} could be assigned to the C—H out-of plane bend mode, and the peak at 1127 cm^{-1} was assigned to the C—H in-plane bend mode [37].

After atrazine was added to the dispersion of CD@Ag-R6G, it would be adsorbed on the surface of CD@Ag through the preferential interaction sites of the nitrogen aromatic atoms [38], which increased the stability of R6G-loaded CD@Ag, and thus achieved a dramatic aggregation of CD@Ag [39]. According to the classical electromagnetic theory, the Raman enhancement efficiency depends on the shape and size of nanoparticles as well as the gaps or junctions between nanoparticles. In the case of aggregated nanoparticles, the large EM-enhanced effect may be attributed to their complex geometries, which provides numerous interstitial gaps between adjacent metallic nanostructures (maybe play the role of electromagnetic “hot-spots"), and thus results in highly efficient Raman scattering [40]. The aggregated CD@Ag ingeniously produced a desirable metal nanostructures with nanogaps to form plentiful “hot spots” with huge electromagnetic field enhancements at junctions [39–42], thus the SERS response of R6G was greatly enhanced (Fig. 3). Moreover, the Raman spectrum of atrazine in the absence and presence of CD@Ag did not show obvious Raman signal, thus atrazine did not interfere with the SERS response of R6G molecule.

3.3. Feasibility of SERS detection for atrazine

In order to achieve highly sensitive SERS detection, the amount of the Raman reporter, R6G, was firstly optimized. The SERS signals of R6G increased with the increasing concentration of R6G for loading. When the concentration of R6G was 1×10^{-7} M, the signals of R6G could be identified clearly, whereas lower concentration did not

produce obvious signal. Thus 1×10^{-7} M R6G was used for detection of atrazine.

The amount of CD@Ag was optimized with a conventional titration protocol by changing the total amount of CD@Ag (i.e., the absolute particle number) in a fixed assay volume of 20 μL at several concentrations of atrazine. As shown in Fig. 4, the SERS responses of R6G at different Raman shifts increased with the increasing atrazine concentration, while the dilution of CD@Ag decreased the responses. Thus the CD@Ag without dilution was used for following detection.

At low concentrations of aggregating agent, a strong repulsion due to Coulomb interaction dominated the potential energy, which led to small aggregation probabilities [43], thus limited the sensitivity of the proposed method. From Fig. 4, it was seen that the SERS responses of R6G decreased when the concentration of atrazine was above 1.0 μM. In this situation, the more atrazine molecules were bounded around the surface of CD@Ag, which led to less binding sites for linking the CD@Ag each other. The threshold concentration of atrazine was changed when the different amounts of CD@Ag were adopted.

The specificity of the proposed system was demonstrated with 3-mercaptopropionic acid and ethambutol. These molecules contain two kinds of functional groups and can be considered as a cross-linker of Ag nanoparticles due to S—Ag or N—H hydrogen bonds. Both 3-mercaptopropionic acid and ethambutol did not show the enhancement of peak intensity of R6G, even at high concentration of 5 μM (Fig. S4). This phenomenon could be attributed to their linear molecule character.

3.4. Analytical performance of the SERS platform

In detectable concentration range, the SERS signals increased with the increasing atrazine concentration (Fig. 5a). A good linear relation occurred between the enhanced times and logarithm value of atrazine concentration ranging from 10 to 1000 nM (Fig. 5b). The correlation coefficient at the Raman shift of 1509.4 cm^{-1} was 0.9940. This method showed high precision (relative standard deviation, RSD = 3%) and accuracy. The limits of detection (LOD) and quantification (LOQ) at 3σ and 10σ according to IUPAC recommendation [44] were estimated to be 5.0 and 10 nM, respectively, which matched with the standard of 0.002 mg/L (about 10 nM) for drinking water quality of China (GB 5749-2006) and WHO defined limit. Compared with some reported methods, including HPLC with diode-array detector (HPLC-DAD), HPLC with mass spectrometry (HPLC-MS), colorimetry, and fluorescent and electrochemical sensors for atrazine detection (Table S1), this proposed SERS method showed higher sensitivity and wider linear range than HPLC-DAD, colorimetric and fluorescent methods. Moreover, this technique could avoid the sample treatment, and the time consumption in both production of immunosensors and electrochemical immunoassay. It possessed attractive analytical features such as simple operation process, wide linear range, high sensitivity and short analysis time.

3.5. Application of the proposed analytical method

Using natural lake water to prepare the practical samples, this presented SERS method was used to detect atrazine spiked in the samples. The results were listed in Table 1, which showed high sensitivity and reasonable recoveries from 95% to 117.5%, indicating good practicability.

4. Conclusion

This work develops a highly sensitive and selective method for the detection of atrazine in aqueous media via SERS technique. This method uses a commonly used Raman molecule R6G as a reporter, whose signal on CD@Ag is greatly enhanced due to the aggregation of nanoparticles, induced by the target atrazine with high efficiency. By taking the advantages of the significant SERS enhancement properties of CD@Ag to R6G, the developed atrazine assay method exhibits excellent analytical performance, such as good specificity, high sensitivity, wide linear range, good accuracy and precision, and acceptable recovery. This simple, rapid, cost-effective sensing system holds great potential for practical application.

Acknowledgements

We gratefully acknowledge the National Natural Science Foundation of China (21635005, 21827812), and the Project Financed by the International Science & Technology Cooperation Plan of Anhui Province (1704e1002225).

Appendix A. Supplementary data

Supplementary data to this article can be found online at https://doi.org/10.1016/j.talanta.2019.03.108.

References

[1] S.B. Huang, J.S. Stanton, Y. Lin, R.A. Yokley, Analytical method for the determination of atrazine and its dealkylated chlorotriazine metabolites in water using SPE sample preparation and GC-MSD analysis, J. Agric. Food Chem. 51 (2003) 7252–7258.
[2] C.D. Nwani, W.S. Lakra, N.S. Nagpure, R. Kumar, B. Kushwaha, S.K. Srivastava, Toxicity of the herbicide atrazine: effects on lipid peroxidation and activities of antioxidant enzymes in the freshwater fish Channa punctatus (Bloch), Int. J. Environ. Res. Public Health 7 (2010) 3298–3312.
[3] K. Grob, I. Kaelin, Attempt for an on-line size exclusion chromatography-gas chromatography method for analyzing pesticide residues in foods, J. Agric. Food Chem. 39 (1991) 1950–1953.
[4] P.P. Qi, Z.W. Wang, G.L. Yang, C.Q. Shang, H. Xu, X. Wang, H. Zhang, Q. Wang, X.Q. Wang, Removal of acidic interferences in multi-pesticides residue analysis of fruits using modified magnetic nanoparticles prior to determination via ultra-HPLC-MS/MS, Microchim. Acta 182 (2015) 2521–2528.
[5] J.P. Li, S.H. Li, X.P. Wei, H.L. Tao, H.C. Pan, Molecularly imprinted electrochemical luminescence sensor based on signal amplification for selective determination of trace gibberellin A3, Anal. Chem. 84 (2012) 9951–9955.
[6] C. Riemenschneider, B. Seiwert, M. Goldstein, M. Al-Raggad, E. Salameh, B. Chefetz, T. Reemtsma, An LC-MS/MS method for the determination of 28 polar environmental contaminants and metabolites in vegetables irrigated with treated municipal wastewater, Anal. Methods 9 (2017) 1273–1281.
[7] E. Zacco, M.I. Pividori, S. Alegret, R. Galve, M.P. Marco, Electrochemical magneto-immunosensing strategy for the detection of pesticides residues, Anal. Chem. 78 (2006) 1780–1788.
[8] J. Sun, L. Gong, Y.T. Lu, D.M. Wang, Z.G. Gong, M.K. Fan, Dual functional PDMS sponge SERS substrate for the on-site detection of pesticides both on fruit surfaces and in juice, Analyst 143 (2018) 2689–2695.
[9] P.L. Stiles, J.A. Dieringer, N.C. Shah, R.P. Van Duyne, Surface-enhanced Raman spectroscopy, Annu. Rev. Anal. Chem. 1 (2008) 601–626.
[10] Q. Huang, X. Zhu, Rapid and large-scale synthesis of pitaya-like silver nanostructures as highly efficient surface-enhanced Raman scattering substrates, Talanta 105 (2013) 117–123.
[11] G. Paul, S. Sarkar, T. Pal, P.K. Das, I. Manna, Concentration and size dependence of nano-silver dispersed water based nanofluids, J. Colloid Interface Sci. 371 (2012) 20–27.
[12] J. Zhang, M.R. Langille, C.A. Mirkin, Synthesis of silver nanorods by low energy excitation of spherical plasmonic seeds, Nano Lett. 11 (2011) 2495–2498.
[13] T. Tetsumoto, Y. Gotoh, T. Ishiwatari, Mechanistic studies on the formation of silver nanowires by a hydrothermal method, J. Colloid Interface Sci. 362 (2011) 267–273.
[14] P. Wang, K. Okamoto, K. Tamada, Tuning the work functions of 2D silver nanoparticle sheets using local oxidation nanolithography, Adv. Mater. Interfaces 1 (2014) 1400268.
[15] Q. Fu, D. Zhang, Y. Chen, X. Wang, L. Han, L. Zhu, P. Wang, H. Ming, Surface enhanced Raman scattering arising from plasmonic interaction between silver nano-cubes and a silver grating, Appl. Phys. Lett. 103 (2013) 041122.
[16] A.L. Swatek, Z. Dong, J. Shaw, M.R. Islam, Self-assembly of silver nanoparticles into dendritic flowers from aqueous solution, J. Exp. Nanosci. 5 (2010) 10–16.
[17] C. Li, H. Ouyang, X. Tang, G. Wen, A. Liang, Z. Jiang, A surface enhanced Raman scattering quantitative analytical platform for detection of trace Cu coupled the catalytic reaction and gold nanoparticle aggregation with label-free Victoria blue B molecular probe, Biosens. Bioelectron. 87 (2017) 888–893.
[18] L. Chen, X. Fu, J. Li, Ultrasensitive surface-enhanced Raman scattering detection of trypsin based on anti-aggregation of 4-mercaptopyridine-functionalized silver nanoparticles: an optical sensing platform toward proteases, Nanoscale 5 (2013) 5905–5911.
[19] M. Reyes, M. Piotrowski, S. Ang, J. Chan, S. He, J. Chu, J. Kah, Exploiting the anti-aggregation of gold nanostars for rapid detection of hand, foot, and mouth disease causing enterovirus 71 using surface-enhanced Raman spectroscopy, Anal. Chem. 89 (2017) 5373–5381.

[20] S. Zhu, Q. Meng, L. Wang, J. Zhang, Y. Song, H. Jin, K. Zhang, H. Sun, H. Wang, B. Yang, Highly photoluminescent carbon dots for multicolor patterning, sensors, and bioimaging, Angew. Chem. Int. Ed. 125 (2013) 4045–4049.
[21] Y. Su, B. Shi, S. Liao, J. Zhao, L. Chen, S. Zhao, Silver nanoparticles/N-doped carbon-dots nanocomposites derived from siraitia grosvenorii and its logic gate and surface-enhanced Raman scattering characteristics, ACS Sustain. Chem. Eng. 4 (2016) 1728–1735.
[22] M. Amjadi, Z. Abolghasemi-Fakhri, T. Hallaj, Carbon dots-silver nanoparticles fluorescence resonance energy transfer system as a novel turn-on fluorescent probe for selective determination of cysteine, J. Photochem. Photobiol. A Chem. 309 (2015) 8–14.
[23] K.M. AbouZeid, M.B. Mohamed, M.S. El-Shall, Hybrid Au–CdSe and Ag–CdSe nanoflowers and core–shell nanocrystals via one-pot heterogeneous nucleation and growth, Small 7 (2011) 3299–3307.
[24] Y. Dong, Q. Wang, L. Wan, X. You, Y. Chi, Carbon based dot capped silver nanoparticles for efficient surface-enhanced Raman scattering, J. Mater. Chem. C 4 (2016) 7472–7477.
[25] H. Luo, C. Gu, W. Zheng, F. Dai, X. Wang, Z. Zheng, Facile synthesis of novel size-controlled antibacterial hybrid spheres using silver nanoparticles loaded with polydopamine spheres, RSC Adv. 5 (2015) 13470–13477.
[26] X. Zhuang, B. Cheng, W. Kang, X. Xu, Electrospun chitosan/gelatin nanofibers containing silver nanoparticles, Carbohydr. Polym. 82 (2010) 524–527.
[27] Z.L. Zhang, X.Y. Zhang, Z.Q. Xin, M.M. Deng, Y.Q. Wen, Y.L. Song, Synthesis of monodisperse silver nanoparticles for ink-jet printed flexible electronics, Nanotechnology 22 (2011) 425601.
[28] B. Yang, X. Chen, R. Liu, B. Liu, C. Jiang, Target induced aggregation of modified Au@Ag nanoparticles for surface enhanced Raman scattering and its ultrasensitive detection of arsenic(III) in aqueous solution, RSC Adv. 5 (2015) 77755–77759.
[29] J. Jin, S. Zhu, Y. Song, H. Zhao, Z. Zhang, Y. Guo, J. Li, W. Song, B. Yang, B. Zhao, Precisely controllable core–shell Ag@carbon dots nanoparticles: Application to in situ super-sensitive monitoring of catalytic reactions, ACS Appl. Mater. Interfaces 8 (2016) 27956–27965.
[30] Y. Hu, Y. Shi, H. Jiang, G. Huang, C. Li, Scalable preparation of ultrathin silica-coated Ag nanoparticles for SERS application, ACS Appl. Mater. Interfaces 5 (2013) 10643–10649.
[31] A. Virga, P. Rivolo, F. Frascella, A. Angelini, E. Descrovi, F. Geobaldo, F. Giorgis, Silver nanoparticles on porous silicon: Approaching single molecule detection in resonant SERS regime, J. Phys. Chem. C 117 (2013) 20139–20145.
[32] E.C. Le Ru, M. Meyer, P.G. Etchegoin, Proof of single-molecule sensitivity in surface enhanced Raman scattering (SERS) by means of a two-analyte technique, J. Phys. Chem. B 110 (2006) 1944–1948.
[33] F.S. Ameer, C.U. Pittman, D. Zhang, Quantification of resonance Raman enhancement factors for rhodamine 6G (R6G) in water and on gold and silver nanoparticles: implications for single-molecule R6G SERS, J. Phys. Chem. C 117 (2013) 27096–27104.
[34] X. Wang, Y. Du, Q. Li, T. Wu, H. Hu, Y. Xu, H. Zhang, Y. Pan, Fabrication of uniform substrate based on silver nanoparticles decorated glycidyl methacrylate-ethylene dimethacrylate porous material for ultrasensitive surface-enhanced Raman scattering detection, J. Raman Spectrosc. 45 (2014) 47–53.
[35] Y.C. Liu, C.-C. Yu, S.F. Sheu, Improved surface-enhanced Raman scattering on optimum electrochemically roughened silver substrates, Anal. Chim. Acta 577 (2006) 271–275.
[36] W.W. Yu, I.M. White, Inkjet printed surface enhanced Raman spectroscopy array on cellulose paper, Anal. Chem. 82 (2010) 9626–9630.
[37] P. Hildebrandt, M. Stockburger, Surface-enhanced resonance Raman spectroscopy of Rhodamine 6G adsorbed on colloidal silver, J. Phys. Chem. 88 (1984) 5935–5944.
[38] S. Bonora, E. Benassi, A. Maris, V. Tugnoli, S. Ottani, M. Di Foggia, Raman and SERS study on atrazine, prometryn and simetryn triazine herbicides, J. Mol. Struct. 1040 (2013) 139–148.
[39] T. Yajima, Y. Yu, M. Futamata, Steric hindrance in cationic and neutral rhodamine 6 G molecules adsorbed on Au nanoparticles, J. Raman Spectrosc. 44 (2013) 406–411.
[40] Y. Liu, Y. Zhang, H. Ding, S. Xu, M. Li, F. Kong, Y. Luo, G. Li, Self-assembly of noble metallic spherical aggregates from monodisperse nanoparticles: their synthesis and pronounced SERS and catalytic properties, J. Mater. Chem. A 1 (2013) 3362–3371.
[41] H. Wei, S.M. Hossein Abtahi, P.J. Vikesland, Plasmonic colorimetric and SERS sensors for environmental analysis, Environ. Sci.: Nano 2 (2015) 120–135.
[42] J.-W. Chen, X.-P. Liu, K.-J. Feng, Y. Liang, J.-H. Jiang, G.-L. Shen, R.-Q. Yu, Detection of adenosine using surface-enhanced Raman scattering based on structure-switching signaling aptamer, Biosens. Bioelectron. 24 (2008) 66–71.
[43] D.P. dos Santos, M.L.A. Temperini, A.G. Brolo, Single-molecule surface-enhanced (Resonance) Raman scattering (SE(R)RS) as a probe for metal colloid aggregation state, J. Phys. Chem. C 120 (2016) 20877–20885.
[44] G. Long, J. Winefordner, Limit of detection. A closer look at the IUPAC definition, Anal. Chem. 55 (1983) 712A–724A.